Title

ABE Condensation over Monometallic Catalysts: Catalyst Characterization and Kinetics

Journal

ChemCatChem, 9(4)

ISSN

1867-3880

Authors

Goulas, Konstantinos A
Gunbas, Gorkem
Dietrich, Paul J
et al.

Publication Date

2017-02-21

DOI

10.1002/cctc.201601507

Peer reviewed

ChemPubSoc Europe

DOI: 10.1002/cctc.201601507

CHEMCATCHEM Full Papers

ABE Condensation over Monometallic Catalysts: Catalyst Characterization and Kinetics

Konstantinos A. Goulas,[a, b, c] Gorkem Gunbas,[a, c, d] Paul J. Dietrich,[e] Sanil Sreekumar,[a, c] Adam Grippo,[c] Justin P. Chen,[b, c] Amit A. Gokhale,[c, e] and F. Dean Toste*[a, c]

Herein, we present work on the catalyst development and the kinetics of acetone-butanol-ethanol (ABE) condensation. After examining multiple combinations of metal and basic catalysts reported in the literature, Cu supported on calcined hydrotalcites (HT) was found to be the optimal catalyst for the ABE condensation. This catalyst gave a six-fold increase in reaction rates over previously reported catalysts. Kinetic analysis of the reaction over CuHT and HT revealed that the rate-determining step is the C–H bond activation of alkoxides that are formed from alcohols on the Cu surface. This step is followed by the addition of the resulting aldehydes to an acetone enolate formed by deprotonation of the acetone over basic sites on the HT surface. The presence of alcohols reduces aldol condensation rates, as a result of the coverage of catalytic sites by alkoxides.

Introduction

Emissions of CO_2 from fossil fuel combustion have been a driving force behind the increase in global temperatures over the last 50 years. As a result, worldwide efforts have been made to reduce CO_2 emissions, culminating in the Kyoto Protocol. As part of its commitments under the Kyoto Protocol, the EU has mandated a minimum bio-derived content in its diesel supply. Currently, biodiesel production primarily relies on vegetable oil to produce fatty acid methyl esters (FAME) derived by transesterification of triglycerides extracted from oleiferous seeds[1,2] or hydrocarbon mixtures obtained by hydrodeoxygenation[1,2] at high temperature and pressure. However, both of these methods are hampered by problems with the vegetable oil supply. In addition to the competition with food supplies, biofuel yields per acre are low in the cases of rapeseed and soybean oil[3] and sustainability issues related to land use have yet to be addressed in the case of palm oil.[4]

In our earlier work, we proposed a strategy combining fermentation and chemical upgrading to yield biodiesel precursor molecules.[5,6] In this sequence, sugars were fermented to a mixture of acetone, butanol, and ethanol that was upgraded to heavier ketones in a dehydrogenation-aldol condensation-hydrogenation reaction pathway. While the ABE condensation reaction was catalyzed by a physical mixtures of Pd/C and K_3PO_4, the water produced during the reaction tended to inhibit the activity of potassium phosphate. Additionally, reaction rates were relatively low (24 h required for complete conversion of the starting material, corresponding to a turnover frequency of about 0.03 h^{-1}) and the use of toluene as a solvent hampered the applicability of this system in an industrial setting. Subsequently, Cu- and Pd-substituted hydrotalcite materials were shown to be efficient catalysts for the ABE condensation. These catalysts showed markedly improved recyclability compared to the original Pd/C-K_3PO_4 system;[7,8] however, the long reaction times, on the order of 20 h (corresponding to a TOF of 0.06 h^{-1}), made this system impractical as an industrial catalyst. In this work, we describe both the improvement of these catalysts by using batch reactor screening and instrumental characterization techniques, such as X-ray absorption spectroscopy, and kinetic studies on the optimal catalysts to determine the reaction pathways.

[a] Dr. K. A. Goulas, Prof. Dr. G. Gunbas, Dr. S. Sreekumar, Prof. Dr. F. D. Toste
Department of Chemistry
University of California, Berkeley
Berkeley, CA 94720 (USA)
E-mail: fdtoste@berkeley.edu

[b] Dr. K. A. Goulas, J. P. Chen
Department of Chemical and Biomolecular Engineering
University of California, Berkeley
Berkeley, CA 94720 (USA)

[c] Dr. K. A. Goulas, Prof. Dr. G. Gunbas, Dr. S. Sreekumar, A. Grippo, J. P. Chen, Dr. A. A. Gokhale, Prof. Dr. F. D. Toste
Energy Biosciences Institute
University of California, Berkeley
Berkeley, CA 94720 (USA)

[d] Prof. Dr. G. Gunbas
Department of Chemistry
Middle East Technical University
Ankara 06800 (Turkey)

[e] Dr. P. J. Dietrich, Dr. A. A. Gokhale
BP Products North America
150 W. Warrenville Road
Naperville, IL 60563 (USA)

Supporting information and the ORCID identification number(s) for the author(s) of this article can be found under http://dx.doi.org/10.1002/cctc.201601507.

This manuscript is part of a Special Issue to celebrate the 50th annual meeting of the German Catalysis Society.

Results and Discussion

Rode et al. showed that alkali-substituted zeolites can be efficient catalysts for aldol condensation reactions of butyraldehyde.[9] We therefore examined Pd-modified CsY and NaY zeolites, as potential catalysts for ABE upgrading. The target products (A–F) of the dehydrogenation/aldol condensation sequence are shown in Scheme 1.

The yield to diesel-range precursors was consistently lower (maximum of 56.8%, Table 1) than that of the hydrotalcite-type materials, which took the reaction to full conversion. It is also worth noting that higher temperatures gave higher yields of etherification products. Ether formation from alcohols is a well-known acid-catalyzed reaction, suggesting that there are residual acid sites on the zeolites. This is undesirable, since, in a commercial process, these oxygenates would be subjected to hydrodeoxygenation to form alkanes. In this process, ethers, such as dibutyl ether, may undergo C–O bond cleavage to form butanes, which are unsuitable for blending with diesel fuel and generally lower in value.

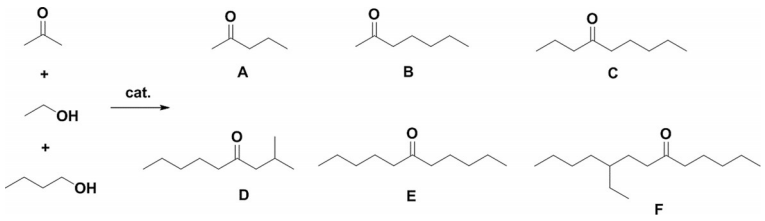

Scheme 1. The ABE condensation reaction.

Table 1. Percent yield of ABE condensation products for the series of Pd-modified, alkali-substituted zeolites. Reaction condition: 2.3 mmol acetone, 3.7 mmol butanol, 1 mmol ethanol, 350 mg catalyst in 1 mL BuOH.

Entry	A	B	C	D	E	F	Total Alcohols	Overall
1Pd/NaY, 200 °C	6.4	14.6	–	–	–	–	–	21.0
2Pd/CsY, 200 °C	4.9	23.3	–	–	–	–	–	28.2
5Pd/CsY, 200 °C	7.6	33.5	–	–	–	–	–	41.1
5Pd/CsY, 215 °C[a]	7.3	47	0.8	0.6	1.1	–	–	56.8
5Pd/CsY, 240 °C[b]	4.9	43.4	1.6	1.2	2.8	–	1.3	55.2

[a] 19 mg butylether formed. [b] 156 mg butylether formed.

Silica-based materials were also investigated as catalysts for the ABE condensation reaction. NaOH and CaO supported on silica have been reported as active catalysts for aldol condensation reactions.[10] Excellent yields were achieved upon supporting Pd on the basified silica catalysts (Table 2). However, the recyclability of these catalysts was rather poor (last three entries in Table 2) in comparison to the previously reported hydrotalcite-based catalysts; the yield of ABE products in the third cycle was less than half of that in the first cycle, compared to a modest 10% loss of ABE yield in the case of hydrotalcite-based catalysts.[7]

It is possible that the water formed in the reaction leaches away the easily-soluble NaOH and $Ca(OH)_2$, and thereby deactivates the catalyst. We also noted the formation of alcohols in the product stream. This observation suggests that there is excess hydrogen in the system, since the formation of the C7 and C11 ketones does not require extra hydrogen. The dehydrogenation of the alcohols in the feed produces one mole of hydrogen, which is consumed again in the hydrogenation of the α,β-unsaturated ketone product of the aldol condensation. Possible pathways for the formation of hydrogen include the Tishchenko reaction and decarbonylation reactions. In the former the dehydrogenation of the hemiacetal produced by the reaction of an aldehyde and an alcohol yields an ester. This pathway has been utilized for the single-step production of ethyl acetate from ethanol.[11–13] In the case of decarbonylation reactions, C–C bond scission is a necessary step in the production of hydrogen from organic oxygenates during reforming over Pt and Pd-based catalysts.[14]

Table 2. Yields of ABE reaction over Na- and Ca-basified SiO_2 catalysts. Reaction conditions: 2.3 mmol acetone, 3.7 mmol butanol, 1 mmol ethanol, 350 mg catalyst in 1 mL BuOH.

Entry	A	B	C	D	E	F	Alcohols	Overall
1Pd/10Na/SiO_2	1.8	26.8	3.2	0.3	22	–	6.0	60.1
0.75Pd/15Na/15Ca/SiO_2	4.8	34.8	5.1	0.6	39.8	1.4	4.7	91.2
0.5Pd/15Na/15Ca/SiO_2	2.5	32.3	6.6	0.5	42.1	2.2	5.0	91.2
0.85Pd/17Na/17Ca/SiO_2	4.1	41.0	4.0	0.9	22.0	0.2	4.7	76.9
1Pd/10Na/10Ca/SiO_2	2.9	34.2	1.7	0.5	10.7	–	4.2	54.2
1Cu/10Na/10Ca/SiO_2	–	20.8	0.4	–	7.1	–	2.9	31.2
0.5Pd/15Na/15Ca/SiO_2, 1st	2.2	31.7	5.4	0.5	38.9	2.0	5.4	86.1
0.5Pd/15Na/15Ca/SiO_2, 2nd	2.9	31.5	1.0	0.4	5.6	–	1.6	43.0
0.5Pd/15Na/15Ca/SiO_2, 3rd	1.9	29.6	0.6	0.3	5.9	–	1.3	39.6

The hydrotalcite-supported metal catalysts studied previously were made on low surface area supports, ranging from 6 to 26 $m^2 g^{-1}$, and we hypothesized that activity could be enhanced by increasing the surface area. To improve the reactivity, the hydrotalcite catalyst was calcined at 823 K prior to the ion exchange step. Consistent with previous studies,[15] this treatment increased the surface area of the raw material up to 200 $m^2 g^{-1}$, indicating the formation of the higher surface area periclase structure. However, reaction studies did not show the expected appreciable improvements in the yield of the reaction (83% vs. 80% for the pre-calcined HT and the control, respectively), or increased selectivity to the C_{11+} fraction of the products. These results are likely a result of the fact that metal oxide reverts to the lamellar structure upon exposure to water[15] during the metal impregnation as indicated by the measured surface area of the finished metal-hydrotalcite material (26 $m^2 g^{-1}$).

It is therefore clear, that to increase the surface area of the catalyst it is necessary to retain the cubic structure of the periclase material. This was achieved by co-precipitating the Cu, Mg and Al hydroxycarbonates from a solution of the nitrates, forming a Cu-doped hydrotalcite, and calcining it to form the high-surface-area periclase structure. Our results (Table S1) indicate that Cu-doped HT materials can be synthesized with

surfaces areas between 140 and 200 $m^2 g^{-1}$ after calcination at 823 K, in agreement with literature reports.[16]

The yields of the ABE condensation reaction using catalysts prepared by coprecipitation are shown in Figure 1. An increase in the yields of ketones A–F was observed with increasing Cu content to approximately 2.5% Cu loading. Furthermore, the selectivity to 2-ethylhexanol and its condensation product with acetone, 4-ethyl-2-nonanone, also increased. Increasing Cu content beyond 2.5% did not result in higher yields, but resulted in increased production of butyl butyrate and decreased formation of 2-ethylhexanol and heavier condensation products. This undesirable effect is likely a result of the formation of a hemiacetal over the basic sites of the HT and its subsequent dehydrogenation by the Cu, as shown in Scheme 2. Cu catalysts are known to catalyze hemiacetal dehydrogenation, formed over basic or amphoteric supports, to form esters.[11–13]

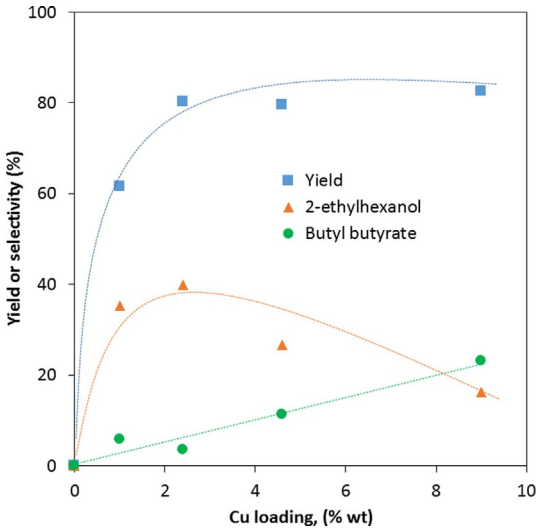

Figure 1. Effects of Cu loading on reaction yield and selectivity. Batch reactor, 513 K, 18 h, 2.3 mmol acetone, 3.7 mmol butanol, 1 mmol ethanol, 350 mg catalyst in 1 mL BuOH. Dashed lines indicate qualitative trends.

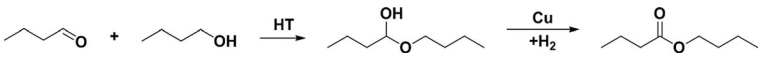

Scheme 2. Esterification of butanol and butyraldehyde.

These results suggest that a balance of acid/base and metal sites is necessary for the selective production of ABE condensation products. This is consistent with the results reported in recent literature [17] for ethanol-to-butadiene conversion, in which group IB metals (Cu, Ag, Au) are supported on MgO-SiO_2 solids. The group IB metals act as redox sites, while the MgO-SiO_2 supports provide acidic and basic sites to catalyze the condensation and dehydration reactions.

Similarly, in our case, Cu provides the sites for the dehydrogenation reaction, while the MgO/Al_2O_3 support provides basic sites for the aldol condensation reaction of acetone with the in situ generated reactive aldehydes.

Another technique employed for high-surface-area HT-supported catalysts is incipient wetness impregnation of metal nitrates on HT.[18] Therefore, 2.5% CuHT catalyst was prepared using an incipient wetness impregnation method; the surface area of the sample was 198 $m^2 g^{-1}$. On testing against the 2.5% CuHT catalyst prepared by coprecipitation, the catalyst prepared by incipient wetness impregnation showed higher yields (Table 3). We posited that co-precipitating the copper nitrate with the magnesium and aluminum nitrates places copper in random positions throughout the structure and not on the surface, where it can be reduced by H_2 and be active for dehydrogenation reactions. To test this hypothesis, the catalyst was characterized using X-ray absorption spectroscopy. The X-ray absorption near edge structure (XANES) results (Figure 2) are consistent with this hypothesis, as the white line decreases in intensity and the edge is shifted to lower photon energies. After treatment in a hydrogen/helium mixture at 523 K, we expect all accessible Cu to be reduced to a Cu^0 species, in accordance with literature TPR data.[19] However, in the case of these catalysts, a significant portion of Cu remains oxidized, in a 2+ oxidation state, and in a coordination environment reminiscent of $Cu(H_2O)_6^{2+}$, as evidenced by the shape of the white line. Cu is therefore octahedrally coordinated in the calcined catalyst, which suggests that Cu substitutes for Mg in the Mg-Al oxide structure and is inaccessible to hydrogen or the alcohols for reduction. This hypothesis is also consistent with literature reports on butadiene production catalysts[17b,c] and our own XPS data, which point to the existence of two distinct Cu^{2+} species (Figure S2).

To understand the reactivity aspects better, additional experiments at short residence times (2 h) were conducted to track the yield and conversion more systematically. To keep the conditions closer to industrial processes, butanol:acetone was limited to a range that was expected to be produced by the fermentation processes, and the use of large excess of butanol solvent was discontinued.. While these conditions resulted in lower conversions (Table 3), they are much more indicative of the suitability of a given catalyst for eventual industrial use. To further increase the aldol condensation rates, we investigated the possibility of using higher alkaline earth element oxides, since these oxides are known to be more basic than MgO and Al_2O_3.[14] Ach-

Table 3. Effects of the solvent, the preparation method and the ratio of substrate to catalyst on the conversion and the yield of 6-undecanone at 513 K, batch reaction. Substrate is ABE mixture.

	Total yield [%]	Yield E [%]	Solvent	substrate/ catalyst [mass]	Reaction time [h]
CuHT (IWI)	89.6	60.4	Butanol	1.25	20
CuHT (Co-Pr)	73.0	35.5	Butanol	1.25	20
CuHT (IWI)	47.5	13.8	None	2	2
CuHT (Co-Pr)	37.8	12.8	None	2	2
CuHT (Ion-exch)	24	2.2	None	2	2

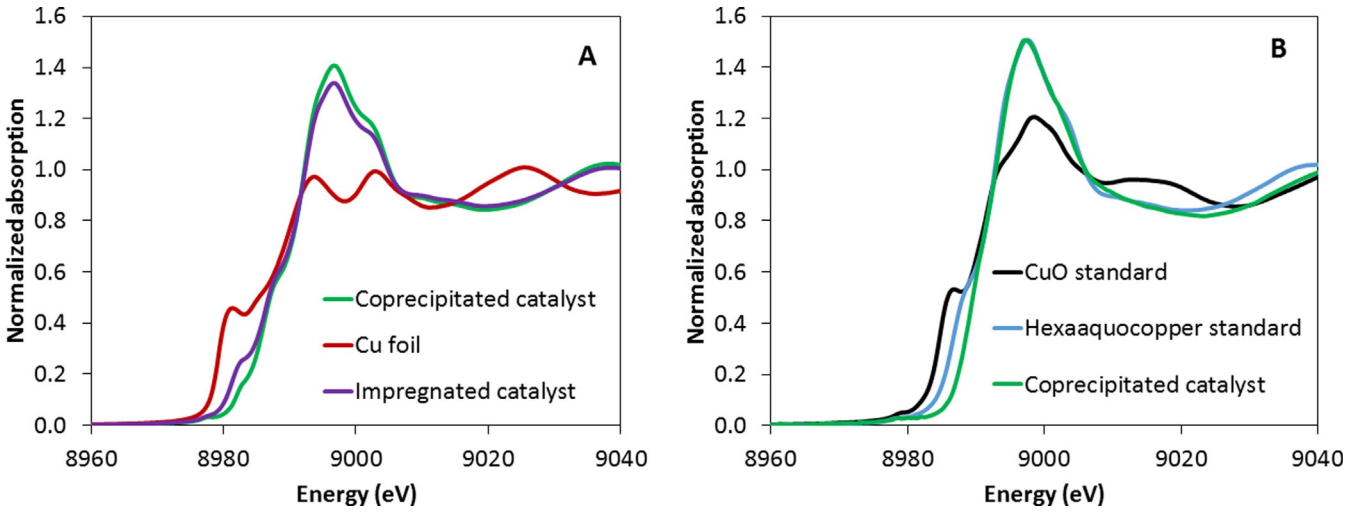

Figure 2. X-ray absorption spectra for 2.5% Cu/HT catalysts and standards. A: Spectra recorded at room temperature in transmission mode after reduction at 523 K under a flowing 50% H_2/He mixture. B: Spectra recorded in fluorescence (Calcined CuHT) and transmission (CuO and catalyst), before reduction, under He at room temperature.

ieving high surface areas for these elements in their pure oxide form is challenging.[20] Hence, these catalysts were supported on SiO_2, using an incipient wetness impregnation of the nitrates, and were calcined at 773 K, with the aim of forming small metal oxide clusters on SiO_2. These materials were then physically mixed with a commercial $Cu/ZnO/Al_2O_3$ catalyst prior to reaction to dehydrogenate the alcohols.

The results of these experiments are shown in Table 4. It is clear that MO/SiO_2 materials behaved poorly, since the product yield was about a third of that of a HT catalyst tested under the same conditions. A possible reason for the poor performance of these materials is that they did not form the cubic MO structure, as evidenced by their X-ray diffractograms which show broad peak attributed to amorphous SiO_2 (Figure S1). The detrimental effects of the formation of silicates for C–C bond formation reactions were reported in the past for butadiene formation reactions.[21]

Table 4. Percent yields for alternative base screening for ABE condensation. 523 K: 4.6 mmol acetone, 7.4 mmol butanol, 2 mmol ethanol, 350 mg basic catalyst in physical mixture with 50 mg $Cu/ZnO/Al_2O_3$. Reaction time 2 hours.

Entry	A	B	C	D	E	F	Total Alcohols	Overall
BaO/SiO_2	–	–	–	–	–	–	–	≈0
MgO/SiO_2	–	–	–	–	–	–	–	≈0
SrO/SiO_2	0.8	6.7	0.2	0.2	–	0.1	–	8.0
CaO/SiO_2	1.9	15.9	0.3	–	0.6	–	0.6	19.3
SrO/MgO (1%)	2.7	17.8	2.6	0.7	11.9	–	1.8	37.5
SrO/MgO (2%)	1.9	13.4	1.6	0.4	7.8	–	1.1	26.2
CaO/MgO (10%)	2.0	12.2	6.3	1.1	28.1	–	3.1	52.8
CaO/MgO (5%)	2.5	15.5	4.2	0.7	19.5	–	2.4	44.8
CaO/MgO (1%)	2.2	10.7	7.1	1.0	27.0	–	5.1	53.1
Hydroxyapatite	2.4	21.3	0.5	0.3	1.3	–	0.2	26
Perovskite	0.5	22.7	0.6	–	5.1	–	4.0	32.9
HT	0.5	6.0	1.6	0.5	20.0	1.8	28.3	58.7

Perovskite and hydroxyapatite are known basic catalysts that have demonstrated effectiveness for other base-catalyzed reactions, such as ethanol oligomerization.[22] Given this, a physical mixture with Cu-containing catalysts was tested in the ABE condensation reaction. Unfortunately, the yields were not high enough (<40%) to warrant further investigations. This is consistent with the observations of Sacia et al.,[23] who showed low activity of these catalysts in the trimerization of methyl ketones at similarly low temperatures.

Doping more basic elements into an MgO structure has been previously proposed as a strategy to improve the basicity of the catalyst and, consequently, the aldol condensation reaction rate.[24,25] On preparation of such oxides from the calcination of the corresponding mixed oxalates,[26] mixed oxides were the dominant phase in low heteroatom substitution percentages (Figures S3 and S5). However, increasing the doping gave rise to another phase, possibly the mixed $(M,Mg)CO_3$ carbonate. It is known that oxalates decompose into carbonates upon heating, with the carbonates decomposing to the oxides upon further heating. TGA experiments (Figure S4 and Figure S6) demonstrated an increase in decomposition temperature with an increase in the atomic number of the substituted group IIA element, suggesting an increase in the fraction of carbonates. Since the carbonates are less basic than the oxides, we hypothesized that the increasing proportion of carbonates in the samples results in the observed reduction of the reaction rate upon increasing the doping over 1%.

To understand the mechanism of the ABE reaction, kinetics of the ABE condensation reactions over both HT and CuHT catalysts were investigated using a gas-phase flow reactor. First, transition-metal-free HT catalysts were used to study the mechanism of the aldol condensation. If acetone and butanol were flowed over the HT catalyst, the cross-coupling product yield at steady state was very low and the effluent was composed mainly of acetone coupling and oligomerization products. This suggests that the transfer (Meerwein-Ponndorf-Verley)[27] hy-

drogenation from the butanol to the acetone is much slower than the formation of the C–C bond. On the contrary, if the butanol feed was spiked with 5% (w/v) butyraldehyde, the main product was the cross-coupling product, 3-hepten-2-one, reflecting the fact that butyraldehyde is a much stronger electrophile than acetone.

These experiments also indicate that butanol adsorbs competitively with acetone on the catalyst surface. At a constant acetone and butyraldehyde pressure, a reduction of rates as butanol pressure increased was observed (Figure 3). This is consistent with earlier reports, which describe a dissociative adsorption of alcohols over metal oxide surfaces to form alkoxides.[28] In this way, unreactive alcohols compete for surface sites with the reactive ketones and aldehydes. To check for the consistency of this model, a Langmuir-Hinshelwood rate law was fit to the dependence of the reaction rate on the butanol. Figure S7 shows that the inverse rate is proportional to the butanol pressure, which is consistent with a Langmuir-Hinshelwood rate model in which the butanol competitively adsorbs on surface sites. This observation matches the ethanol inhibition effects reported by Young et al. during ethanol Guerbet catalysis over TiO_2.[29] Also, Ho et al. reported that ethanol adsorbs competitively over hydroxyapatite catalysts during the same reaction.[30] The apparent activation energy for the aldol condensation reaction over HT is 27 kJ mol^{-1}, as seen from the slope of Figure S8.

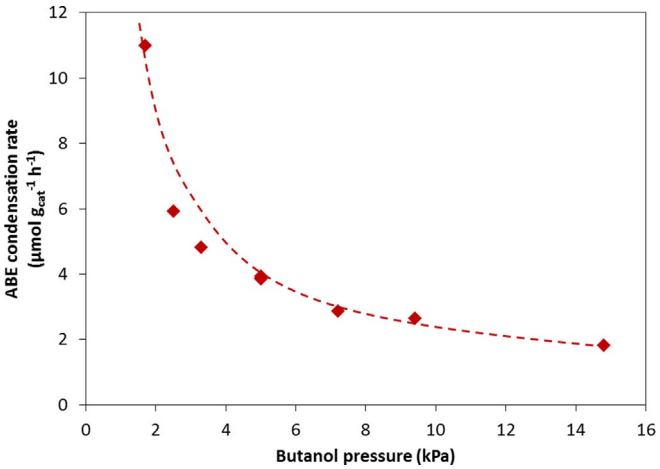

Figure 3. Effects of butanol pressure on aldol condensation rate. Gas-phase flow reactor, 0.4 kPa butyraldehyde, 2 kPa acetone, 2.5% Cu/HT catalyst, 473 K.

As shown in Scheme 3, aldol condensation reactions over basic catalysts are generally believed to take place via the abstraction of a proton in the position alpha to the carbonyl to form an enolate, followed by an attack of the electron-rich enolate onto the electrophilic carbonyl carbon. Wang et al. demonstrated that the enolate formation over anatase TiO_2 was rate-determining of the aldol condensation reaction of propionaldehyde and acetone,[31] while Shylesh et al. found that the enolate formation step was equilibrated during acetone and other methyl ketone trimerization reactions over calcined hydrotalcite.[32] In the ABE condensation, the regioselectivity of the ABE products is consistent with the enolate formation primarily occurring from acetone. Only 2-heptanone and its unsaturated counterpart, 3-hepten-2-one are observed. The rate of the coupling reaction between acetone and butyraldehyde shows a first-order dependence on acetone (Figure 4A) and the dependence on butyraldehyde is also first-order (Figure 4B). These observations support reversible enolate formation; an irreversible enolate formation step would result in an aldol condensation rate independent of butyraldehyde pressure.

Furthermore, the observed KIE with [D_6]acetone ($k_H/k_D = 2.4$) is consistent with the rate-determining step for the aldol condensation involving the activation of a C–H or O–H bond. The apparent contradiction with the results of Shylesh et al.,[32] who showed a KIE equal to 0.96 with [D_6]acetone, can be explained by the fact that butyraldehyde is a much stronger electrophile than acetone, resulting in a much more facile C–C bond formation in the case of the ABE condensation. As such, the rate-determining step in the sequence is the associative desorption of the ketol or the dehydration of the ketol. To distinguish between those two possibilities, we prepared the ketol ex situ and fed it over the HT catalyst. No ketol was detected in the effluent of the reactor, indicating that the ketol was rapidly decomposed over the catalyst, thereby ruling the dehydration out as a rate-determining step. As such, we conclude that the concerted abstraction of a proton from the sur-

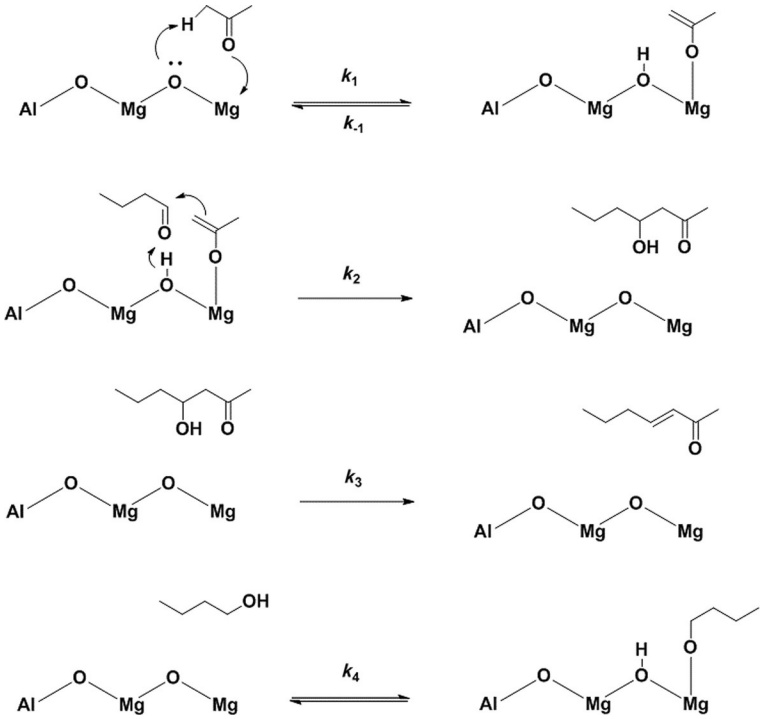

Scheme 3. Condensation of acetone and butyraldehyde over a MgAlO surface.

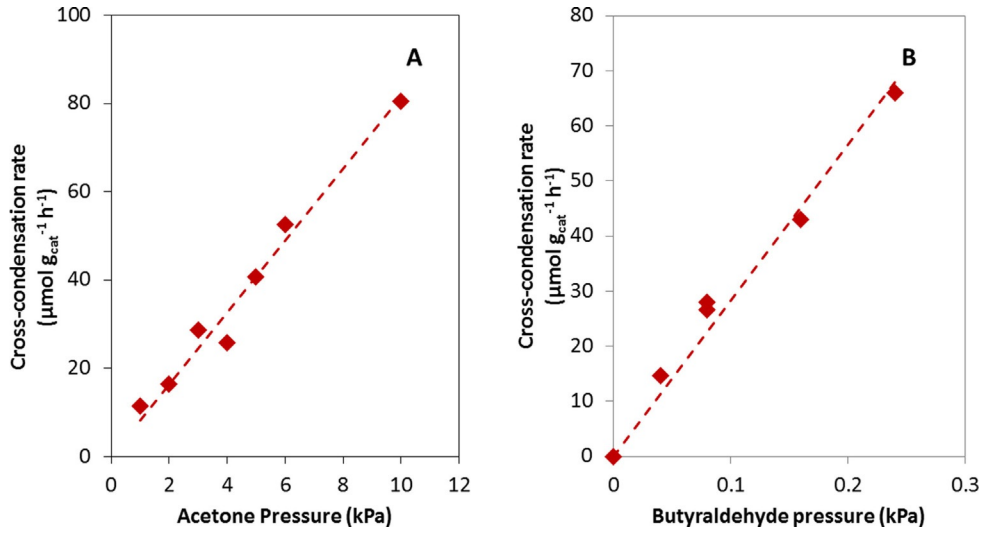

Figure 4. Dependence of cross-condensation rate on acetone pressure (A) and butyraldehyde pressure (B). 473 K, HT catalyst, 0.4 kPa butyraldehyde, 2 kPa acetone.

face to form the ketol is most likely the rate determining step of the aldol condensation.

For the CuHT catalysts, we studied a representative 2.5% Cu/HT catalyst. The butanol dehydrogenation rate is proportional to the butanol partial pressure at the low-pressure regime (Figure 5). This is consistent with an earlier report for isopropanol dehydrogenation over Cu/C catalysts, in which Rioux and Vannice[33] suggested that the rate-determining step for alcohol dehydrogenation over Cu surfaces is the O–H bond activation. To test this hypothesis, we compared the dehydrogenation rates for butanol and butanol-OD. We observed a KIE equal to 1.1, which is inconsistent with an O–H bond scission as the rate-determining step. This suggests that the C–H bond activation is the rate-determining step for the dehydrogenation of butanol on Cu surfaces. This is consistent with the TPD studies of Bowker and Madix, who showed that O-H activation and alkoxide formation occurs over Cu surfaces at low temperatures, as opposed to C–H bond activation, which occurs at higher temperatures.[34,35]

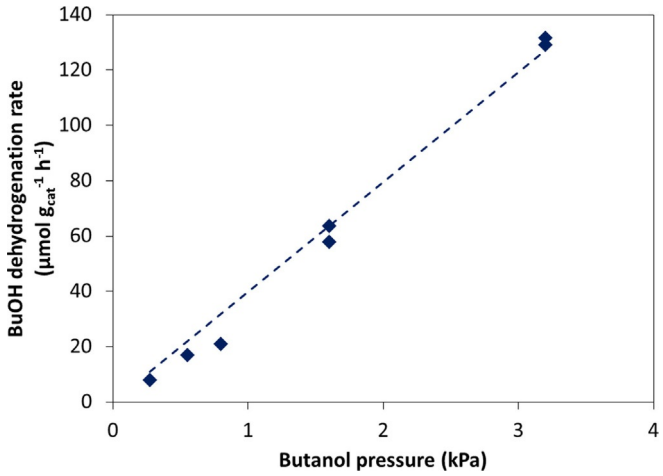

Figure 5. Dependence of butanol dehydrogenation on butanol pressure. 2.5% Cu/HT IWI, 473 K, 2.5 kPa acetone, balance He.

Conclusions

In this work, we have examined a number of base-supported metal catalysts for the condensation of acetone with butanol and ethanol to form drop-in diesel fuel precursor ketones. Considerable improvements of the reaction rates were achieved by increasing the surface area of hydrotalcite-supported Cu catalysts. Additionally, we showed that supporting Cu onto calcined hydrotalcite materials by incipient wetness impregnation gave catalysts that were tuned to give high selectivity to the ABE ketones without extensive formation of undesirable ester byproducts. Alcohol dehydrogenation rates over the Cu surfaces are proportional to the alcohol pressure and do not show any kinetic isotope effect with butanol-OD. This observation suggests that the rate-determining step of the dehydrogenation is the C–H bond cleavage. On the other hand, the aldol condensation of butyraldehyde with acetone proceeds over the HT surface via an equilibrated enolate formation, followed by a rate-limiting surface proton abstraction to form the ketol. The ketol is then rapidly dehydrated to form the unsaturated ketone.

Experimental Section

Pd-modified Y zeolite[8] and Na/Ca/SiO_2-supported Pd[9] were prepared based on methods described in detail elsewhere in the literature. Preparation of mixed $M_xMg_{1-x}O$ oxides, where M is Ca or Sr, was achieved by a variation of the method proposed by Putanov et al., whereby magnesium oxalate is precipitated from a magnesium acetate solution upon addition of oxalic acid.[26] In our experiments, we added a 0.83 M solution of oxalic acid (1.2 equivalents) to a 25 wt% magnesium acetate solution, spiked with calcium or strontium acetate. The resulting milky suspension was aged for 16 h and subsequently the solids filtered and dried in vacuo at

343 K. Calcination of the mixed oxalates at 773 K (5 K min^{-1}, 4 h) afforded mixed oxides.

Coprecipitated Cu catalysts were prepared by modifying the procedure outlined by Climent et al.[36] In this procedure, a solution of magnesium and aluminum nitrates (1.5 M total metal concentration, 3:1 mol Mg:Al) was mixed with a copper and aluminum nitrate solution (1.5 M total metal concentration, 3:1 mol Cu:Al). The resulting solution was heated to 333 K and an equal volume of a solution of ammonium hydroxide (3.375 M) and ammonium carbonate (1 M) was added to it dropwise. The resulting slurry was stirred overnight and the solids filtered and washed with a volume of distilled water equal to five times the volume of the solution. After drying at ambient air at 373 K, the solids were treated in ambient air at 823 K for 4 h (ramp rate 1 K min^{-1}). NiHT and CoHT catalysts were prepared in a similar way, using $Ni(NO_3)_2{\cdot}6H_2O$ and $Co(NO_3)_2{\cdot}6H_2O$, respectively, in the place of copper nitrate hemipentahydrate.

Hydrotalcite-supported Cu catalysts were also prepared by incipient wetness impregnation of a solution of copper nitrate hemipentahydrate into a mixed magnesium-aluminum oxide. This oxide was prepared by calcination of synthetic hydrotalcite (Sigma–Aldrich) at 823 K for 4 h (ramp rate 1 K min^{-1}). Following impregnation, the catalyst precursor was dried in ambient air at 373 K and subsequently calcined at 823 K for 4 h (ramp rate 1 K min^{-1}). For the preparation of Pd/HT catalysts, a similar procedure was followed, using palladium nitrate hydrate (Sigma Aldrich). For RuHT, the calcined hydrotalcite was impregnated with an aqueous solution of $RuCl_3$ and calcined, whereas for PtHT, the calcined hydrotalcite was impregnated with an aqueous solution of H_2PtCl_6 and reduced at 723 K in H_2 for 2 h (ramp 2 K min^{-1}) after drying at 373 K overnight. Titanium dioxide was prepared following a procedure reported by Wang and Ying.[33] A mixture of ethanol and water was added dropwise to a titanium isopropoxide solution in ethanol. The ratio of titanium isopropoxide to water was 1:100. After hydrolysis, the resulting suspension was aged for 16 h at ambient temperature. The solids were separated by filtration and dried in stagnant ambient air at 373 K for 16 h.

Hydroxyapatite was prepared according to Wang, et al.[37] In this process, a stoichiometric quantity of an ammonium hydrogen phosphate solution was added dropwise at ambient temperature to a calcium nitrate solution, for which pH was adjusted to 11 with aqueous ammonium hydroxide solution. The slurry was aged at 363 K for 1 h and the solids were subsequently filtered and washed with copious amounts of water. After that, they were treated in ambient air at 373 K for at least 16 h and subsequently treated for 4 h at 573 K (ramp rate 5 K min^{-1}).

Surface areas of the catalysts were measured by means of nitrogen physisorption using a Micromeritics Tristar 3000 analyzer. The data were analyzed using the BET and BJH methods for surface area and pore size, respectively. The structure of the catalysts was investigated by X-ray diffraction (XRD) and X-ray absorption spectroscopy (XAS). XRD experiments were performed using a Bruker D8 instrument using a 2θ-θ geometry, scanning from $2\theta = 20^{o}$ to 60°, at a rate of 0.02 °s^{-}. Thermogravimetric analysis of the catalysts was performed using a TA8020 TGA instrument, using a 5 K min^{-1} ramp to 1123 K under air flow. Alumina crucibles were used to hold 20–40 mg of sample.

X-ray absorption spectroscopy experiments were performed on the Sector 10, Materials Research Collaborative Access Team, Insertion Device (ID) and bending magnet (BM) beamlines at the Advanced Photon Source, Argonne National Lab. Experiments were conducted at the Pd K (24350 eV) and Cu K (8979 eV) edges. Experiments were performed in either transmission (Pd and Cu) or fluorescence (Cu) detection modes. A series of 3 ion chambers were used, with the third detector simultaneously measuring a reference foil with all experiments for energy calibration. A Lytle detector was used as the fluorescence detector. For transmission experiments, samples were packed into self-supporting wafers, in a 6-well sample holder. Sample loading was calculated to give an absorbance (μ_x) of <2.5 to avoid self-absorption effects, and an edge step ($\Delta\mu_x$) between 0.2 and 1.5. Fluorescence samples were packed into self-supporting wafers in a custom fluorescence holder that held the sample at a 45° angle incident to the beam path. The detector was placed at a 90° angle incident to the beam path.

X-ray photoelectron spectroscopy (XPS) experiments were performed at the Surface Analysis Facility of the University of Delaware. A Thermo Scientific Kalpha+ instrument, with an $Al_{K\alpha}$ source was used for the experiments. The analysis chamber pressure was maintained at 5×10–8 mbar or lower and the spot size was 0.4 mm in diameter. The samples were placed on conductive carbon tape and the analyses were conducted with the electron flood gun on to minimize charging effects.

Samples were contained in 1″ OD quartz tubes connected to Ultratorr fittings with welded ball valves at the end to control the gas atmosphere. For fluorescence experiments, a similar 1″ OD quartz tube with a cone attached to the side was used. The samples were then reduced in situ using a 50% H_2/He gas mixture at the prescribed temperature. Samples were held for 0.5–1 h (reducing time was determined to not have an effect on the final state), at 523 K after which the gas flow was switched to He (Ultra High Purity grade) for 10–15 min. The samples were then cooled to room temperature and scanned at room temperature under a static He atmosphere.

In all reaction experiments, we used an E:A:B = 1:3:6 (by weight) ratio for ethanol, acetone and butanol mixing, since this is the ratio produced by C. acetobutylicum during fermentation. Batch reactions were conducted in pressure tubes (Q-Tubes), using a procedure described in detail elsewhere.[6,7] Gas-phase reactions were conducted in a tubular fused silica reactor with plug-flow hydrodynamics. In this reactor, the catalyst was supported on a quartz frit. Before reaction, the catalyst was sieved down to a size under 180 μm to avoid mass transfer effects during reaction. The reactor was enclosed in a furnace (ATS Pennsylvania) with aluminum inserts and the temperature was controlled by a PID controller (Watlow). Gas flow through the catalyst was regulated using mass flow controllers (Parker). Liquid reactants were vaporized into the gas stream through a syringe port in the heated transfer lines. Their flow was regulated by a syringe pump (Legato 100).The effluent of the reactor was analyzed online using a gas chromatograph (Shimadzu GC 2014) equipped with a flame ionization detector and an HP-1 capillary column.

Acknowledgements

This research was funded by BP through the Energy Biosciences Institute. MRCAT operations are supported by the Department of Energy and the MRCAT member institutions. This research used resources of the Advanced Photon Source, a U.S. Department of Energy (DOE) Office of Science User Facility operated for the DOE Office of Science by Argonne National Laboratory under Contract

No. DE-AC02-06CH11357. We also acknowledge NSF grant 1428149 for XPS analysis.

Keywords: ABE · aldol condensation · copper · hydrotalcite · kinetic isotope effect

[1] "Triglycerides and Oils for Biofuels": D. Y. Murzin, P. Mäki-Arvela, I. L. Simakova, *Kirk-Othmer Encyclopedia of Chemical Technology*, **2012**, pp. 1–14, John Wiley & Sons, Hoboken.
[2] P. Mäki-Arvela, I. Kubickova, M. Snåre, K. Eränen, D. Y. Murzin, *Energy Fuels* **2007**, *21*, 30–41.
[3] C. Somerville, *Curr. Biol.* **2007**, *17*, R115–R119.
[4] a) B. Wicke, V. Dornburg, M. Junginger, A. Faaij, *Biomass Bioenergy* **2008**, *32*, 1322–1337; b) L. P. Koh, D. S. Wilcove, *Nature* **2007**, *448*, 993–994.
[5] a) T. J. Schwartz, B. J. O'Neil, B. H. Chanks, J. A. Dumesic, *ACS Catal.* **2014**, *4*, 2060–2069; b) A. Deneyer, T. Renders, J. Van Aelst, S. Van den Soch, D. Gabriëls, B. Sels, *Curr. Opin. Chem. Biol.* **2015**, *29*, 40–48; c) K. A. Goulas, F. D. Toste, *Curr. Opin. Biotechnol.* **2016**, *38*, 47–53; d) T. J. Schwartz, B. H. Shanks, J. A. Dumesic, *Curr. Opin. Biotechnol.* **2016**, *38*, 54–62; e) L. Wu, T. Moteki, A. A. Gokhale, D. W. Flaherty, F. D. Toste, *Chem* **2016**, *1*, 32–58; f) Y. Huo, H. Zeng, Y. Zhang, *ChemSusChem* **2016**, *9*, 1078–1080.
[6] a) P. Anbarasan, Z. C. Baer, S. Sreekumar, E. Gross, J. B. Binder, H. W. Blanch, D. S. Clark, F. D. Toste, *Nature* **2012**, *491*, 235–239; b) S. Sreekumar, Z. C. Baer, A. Pazhamalai, G. Gunbas, A. Grippo, H. W. Blanch, D. S. Clark, F. D. Toste, *Nat. Protoc.* **2015**, *10*, 528–537; c) K. A. Goulas, S. Sreekumar, Y. Song, P. Kharidehal, G. Gunbas, P. J. Dietrich, G. R. Johnson, Y. C. Wang, A. M. Grippo, L. C. Grabow, A. A. Gokhale, F. D. Toste, *J. Am. Chem. Soc.* **2016**, *138*, 6805–6812.
[7] a) S. Sreekumar, Z. C. Baer, E. Gross, S. Padmanaban, K. A. Goulas, G. Gunbas, S. Alayoglu, H. W. Blanch, D. S. Clark, F. D. Toste, *ChemSusChem* **2014**, *7*, 2445–2448.
[8] For subsequently reported catalyst systems for ABE condensation: a) S. Nahreen, R. B. Gupta, *Energy Fuels* **2013**, *27*, 2116–2125; b) S. B. Bankar, S. A. Survase, H. Ojamo, T. Granström, *Bioresour. Technol.* **2013**, *140*, 269–276; c) G. Xu, Q. Li, J. Feng, Q. Liu, Z. Zhang, X. Wang, X. Zhang, X. Mu, *ChemSusChem* **2014**, *7*, 105–109; d) G. Onyestyák, Gy. Novodárszki, A. F. Wellisch, A. Pilbáth, *Catal. Sci. Technol.* **2016**, *6*, 4516–4524; e) H. T. VO, S. M. Yeo, D. Dahnum, J. Jae, C. S. Hong, H. Lee, *Chem. Eng. J.* **2016**, DOI: 10.1016/j.cej.2016.11.044.
[9] E. J. Rode, P. E. Gee, L. N. Marquez, T. Uemura, M. Bazargani, *Catal. Lett.* **1991**, *9*, 103–113.
[10] C. A. Hamilton, *Appl. Catal. A* **2004**, *263*, 63–70.
[11] K. Inui, T. Kurabayashi, S. Sato, *J. Catal.* **2002**, *212*, 207–215.
[12] A. B. Gaspar, F. G. Barbosa, S. Letichevsky, L. G. Appel, *Appl. Catal. A* **2010**, *380*, 113–117.
[13] N. Iwasa, N. Takezawa, *Bull. Chem. Soc. Jpn.* **1991**, *64*, 2619–2623.
[14] a) D. A. Simonetti, E. L. Kunkes, J. A. Dumesic, *J. Catal.* **2007**, *247*, 298–306; b) G. W. Huber, R. D. Cortright, J. A. Dumesic, *Angew. Chem. Int. Ed.* **2004**, *43*, 1549–1551; *Angew. Chem.* **2004**, *116*, 1575–1577.
[15] D. P. Debecker, E. M. Gaigneaux, G. Busca, *Chem. Eur. J.* **2009**, *15*, 3920–3935 and references therein.
[16] V. Rives, S. Kannan, *J. Mater. Chem.* **2000**, *10*, 489–495.
[17] a) S. Shylesh, A. A. Gokhale, C. D. Scown, D. Kim, C. R. Ho, A. T. Bell, *ChemSusChem* **2016**, *9*, 1462–1472; b) C. Angelici, F. Meirer, A. M. J. van der Eerden, H. L. Schaink, A. Goryachev, J. P. Hofmann, E. J. M. Hensen, B. M. Weckhuysen, P. C. A. Bruijnincx, *ACS Catal.* **2015**, *5*, 6005–6015; c) C. Angelici, M. E. Z. Velthoen, B. M. Weckhuysen, P. C. A. Bruijnincx, *ChemSusChem* **2014**, *7*, 2505–2515; d) W. Janssens, E. V. Makshina, P. Vanelderen, F. De Clippel, K. Houthoofd, S. Kerkhofs, J. A. Martens, P. A. Jacobs, B. F. Sels, *ChemSusChem* **2015**, *8*, 994–1008.
[18] K. O. Christensen, D. Chen, R. Lødeng, A. Holmen, *Appl. Catal. A* **2006**, *314*, 9–22.
[19] S. Galvagno, C. Crisafulli, R. Maggiore, A. Giannetto, J. Schwank, *J. Therm. Anal.* **1987**, *32*, 471–483.
[20] G. Zhang, H. Hattori, K. Tanabe, *Appl. Catal.* **1988**, *36*, 189–197.
[21] G. Natta, R. Rigamonti, *Chim. Ind.* **1947**, *29*, 239–243.
[22] J. T. Kozlowski, R. J. Davis, *ACS Catal.* **2013**, *3*, 1588–1600.
[23] a) E. R. Sacia, B. Madhesan, M. H. Deaner, K. A. Goulas, F. D. Toste, A. T. Bell, *ChemSusChem* **2015**, *8*, 1726–1736; b) S. Sreekumar, M. Balakrishnan, K. A. Goulas, G. Gunbas, A. A. Gokhale, Y. L. Louie, A. Grippo, C. D. Scown, A. T. Bell, F. D. Toste, *ChemSusChem* **2015**, *8*, 2609–2614; c) M. Balakrishnan, E. R. Sacia, S. Sreekumar, G. Gunbas, A. A. Gokhale, C. D. Scown, F. D. Toste, A. T. Bell, *Proc. Natl. Acad. Sci. USA* **2015**, *112*, 7645–7649.
[24] J. I. Di Cosimo, V. K. Díez, C. R. Apesteguía, *Appl. Catal. A* **1996**, *137*, 149–166.
[25] W. Q. Shen, G. A. Tompsett, R. Xing, W. C. Conner, G. W. Huber, *J. Catal.* **2012**, *286*, 248–259.
[26] P. Putanov, E. Kis, G. Boskovic, K. Lazar, *Appl. Catal.* **1991**, *73*, 17–26.
[27] P. S. Kumbhar, J. Sanchez-Valente, J. Lopez, F. Figueras, *Chem. Commun.* **1998**, 535–536.
[28] M. A. Barteau, *Chem. Rev.* **1996**, *96*, 1413–1430 and references therein.
[29] Z. D. Young, S. Hanspal, R. J. Davis, *ACS Catal.* **2016**, *6*, 3193–3202.
[30] C. R. Ho, S. Shylesh, A. T. Bell, *ACS Catal.* **2016**, *6*, 939–948.
[31] S. Wang, K. Goulas, E. Iglesia, *J. Catal.* **2016**, *340*, 302–320.
[32] S. Shylesh, D. Kim, A. A. Gokhale, C. G. Canlas, J. O. Struppe, C. R. Ho, D. Jadhav, A. Yeh, A. T. Bell, *Ind. Eng. Chem. Res.* **2016**, *55*, 10635–10644.
[33] R. M. Rioux, M. A. Vannice, *J. Catal.* **2003**, *216*, 362–376.
[34] M. Bowker, R. J. Madix, *Surf. Sci.* **1980**, *95*, 190–206.
[35] M. Bowker, R. J. Madix, *Surf. Sci.* **1982**, *116*, 549–572.
[36] M. J. Climent, A. Corma, S. Iborra, A. Velty, *J. Catal.* **2004**, *221*, 474–482.
[37] K. Wang, G. J. Kennedy, R. A. Cook, *J. Mol. Catal. A* **2009**, *298*, 88–93.

Manuscript received: November 23, 2016
Revised: January 9, 2017
Accepted Article published: January 9, 2017
Final Article published: February 9, 2017